This notion is consistent with the description by McQueen et al. (2), that the metastable α-PbO_2 phase at ambient conditions was transformed back to rutile by heating at 400°C. The rutile → α-PbO_2 type transition may be a reconstructive-type transition with large atomic displacement (15).

Thus, our work indicates that the first transition observed by Syono et al. (4) corresponds to the formation of the baddeleyite phase and that the second transition, around 100 GPa, may correspond to the pressure-induced transition already observed in ZrO_2.

REFERENCES AND NOTES

1. See, for example, L. Liu and W. A. Bassett, Elements, Oxides, and Silicates (Oxford Univ. Press and Clarendon Press, New York and Oxford, 1982), pp. 92–195.
2. R. G. McQueen et al., Science 155, 1401 (1967).
3. T. Mashimo, K. Nagayama, A. Sawaoka, J. Appl. Phys. 54, 5043 (1983).
4. Y. Syono, K. Kusaba, M. Kikuchi, K. Fukuoka, T. Goto, in High-Pressure Research in Mineral Physics, M. H. Manghnani and Y. Syono, Eds. (Terra Scientific, Tokyo, 1987), pp. 385–392.
5. L. V. Al'tshuler, M. A. Podurets, G. V. Simakov, R. F. Trunin, Sov. Phys. Solid State 15, 969 (1973).
6. L. Liu, Science 199, 422 (1978).
7. L. C. Ming and M. H. Manghnani, High-Pressure Research in Geophysics, S. Akimoto and M. H. Manghnani, Eds. (Center for Academic Publications Japan/Tokyo and Reidel/Dordrecht, 1982), pp. 329–347.
8. The method is almost the same as that adopted for the observation of the high-pressure transitions in SnO_2 by S. Endo et al. [High Press. Res. 4, 408 (1990)]. The cubic press, MAX80, at the National Laboratory for High Energy Physics was mainly used. A boron-epoxy cell was used as a pressure medium, and the pressure was calibrated on the basis of the compression of NaCl and Au at room temperature. High temperature was generated by a graphite heater inserted in a cell and measured by a Pt-Pt13Rh thermocouple.
9. Y. Sato, in High-Pressure Research: Applications in Geophysics, M. H. Manghnani and S. Akimoto, Eds. (Academic Press, New York, 1977), pp. 307–323.
10. L. Ming and M. H. Manghnani, J. Geophys. Res. 84, 4777 (1979).
11. R. W. G. Wyckoff, Crystal Structures (Interscience, New York, ed. 2, 1963), vol. 1, pp. 239–444.
12. J. C. Jamieson and B. Olinger, Science 161, 893 (1968).
13. J. F. Mammone, S. K. Sharma, M. Nicol, Solid State Commun. 34, 799 (1980).
14. M. Akaogi et al., in Program and Abstracts of Papers of 30th High-Pressure Conference of Japan, Y. Syono, Ed. (Sendai, Japan, 1989), pp. 166–167 (in Japanese).
15. See, for example, K. Kusaba, M. Kikuchi, K. Fukuoka, Y. Syono, Phys. Chem. Miner. 15, 238 (1988).
16. Powder Diffraction File (JCPDS International Center for Diffraction Data, Swarthmore, PA), Inorganic 13-307 and 24-1165.

28 August 1990; 12 December 1990

Endothelial Expression of a Mononuclear Leukocyte Adhesion Molecule During Atherogenesis

MYRON I. CYBULSKY* AND MICHAEL A. GIMBRONE, JR.

An inducible rabbit endothelial adhesion molecule that is selective for mononuclear leukocytes has been identified. This adhesion protein was expressed on the surface of activated cultured endothelium in two forms, 118 and 98 kilodaltons, the amino-terminal sequence of each being highly homologous to human VCAM-1. In dietary hypercholesterolemic and Watanabe heritable hyperlipidemic rabbit models of atherosclerosis, this adhesion molecule was found to be expressed in a localized fashion by aortic endothelium that overlies early foam cell lesions. This lesion-localized expression suggests a potential endothelium-dependent mechanism for mononuclear leukocyte recruitment during atherogenesis and may provide a molecular marker for early atherosclerosis.

T HE PATHOGENESIS OF AN ATHEROsclerotic plaque is a complex and chronic process that involves the focal accumulation of lipid, leukocytes, smooth muscle cells, and extracellular matrix in the intima of large arteries. Adherence of circulating monocytes and lymphocytes to the arterial endothelial lining is one of the earliest detectable events in human and experimental atherosclerosis (1). The subsequent transendothelial migration of these adherent leukocytes, their accumulation in the intima, transformation of monocytes into lipid-engorged "foam cells," and secretion of cytokines and growth factors are important events in the initiation and progression of atherosclerotic plaques (1). As atherosclerotic plaques increase in size, mononuclear leukocyte recruitment continues to be evident, predominantly at the plaque borders (1, 2). The localized nature and mononuclear leukocyte specificity of these cellular interactions may, in part, be a consequence of changes in the adhesive properties of the endothelial surface that involve the expression of "ATHERO-ELAMs" (inducible endothelial-leukocyte

adhesion molecules that are expressed in atherosclerotic plaques). With the use of an in vitro cell culture model and a monoclonal antibody (MAb) strategy, we have now identified, immunochemically characterized, and purified a protein from lipopolysaccharide (LPS)-activated rabbit endothelial cells (ECs) that functions as a mononuclear leukocyte–selective adhesion molecule. The localization of this molecule in developing atherosclerotic lesions suggests a potential pathogenic role.

We searched for ATHERO-ELAMs in the rabbit because dietary and heritable models of atherosclerosis are well described in this animal (3). We established EC cultures from the aorta and inferior vena cava of normal New Zealand White rabbits (4) in order to study leukocyte-EC interactions. Treatment of ECs with bacterial endotoxin (LPS) induced a protein synthesis–requiring hyperadhesive surface change, which was quantitated (5) with cells of the U937 human myelomonocytic line (6) (Fig. 1, A and B). MAbs were generated to LPS-activated ECs (7), and we selected three of these antibodies—which are designated Rb1/9,

Vascular Research Division, Departments of Pathology, Brigham and Women's Hospital and Harvard Medical School, Boston, MA 02115.

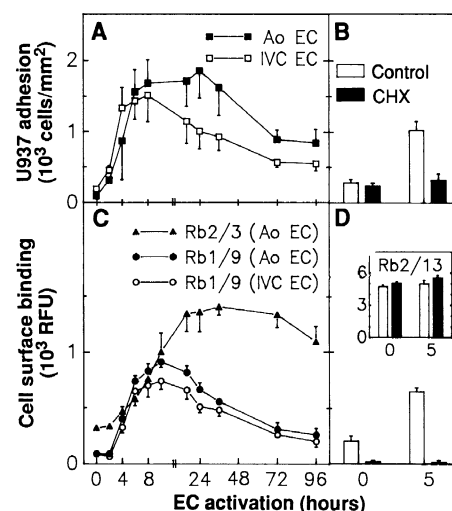*To whom correspondence should be addressed.

Fig. 1. U937 cell adhesion (A and B) and specific MAb binding (C and D) to EC monolayers (passage 2) derived from the aorta (Ao) and inferior vena cava (IVC) of the same New Zealand White rabbit. Activation of ECs with LPS (Escherichia coli; 1 μg/ml) increased both U937 cell adhesion (A) and MAb binding (C) in a time-dependent manner. The binding profile of MAb Rb1/9 was similar to the EC adhesive change for U937 cells, whereas Rb2/3 recognized a surface epitope with higher basal expression and a sustained LPS-induced expression. Rb2/4 binding was virtually identical to that of Rb1/9 (12). Cycloheximide (CHX) (10 μg/ml) abolished the LPS-induced increase in U937 cell adhesion (B) and Rb1/9 cell surface binding (D) during a 5-hour incubation of IVC ECs with LPS. CHX did not affect either the integrity of EC monolayers or the binding of MAb Rb2/13 (specific for an abundant constitutive EC antigen) (D, inset). In each case, data points represent the mean ± SD of quadruplicate measurements.

Rb2/3, and Rb2/4 and are all immunoglobulin G₁ (IgG₁)—for their ability to recognize LPS-inducible EC surface antigens in cell surface fluorescence immunoassays (Fig. 1, C and D).

The leukocyte-adhesive function of these inducible EC surface antigens was assessed with EC monolayers that had been treated with LPS for 18 hours. In adhesion assays performed at 4°C, saturating concentrations of Rb1/9 F(ab')₂ significantly inhibited the adhesion of U937, HL-60, and THP-1 cell lines, as well as that of elutriated human blood monocytes and lymphocytes (Fig. 2). The adhesion of U937 and HL-60 cells was also inhibited in assays performed at 37°C. Decreased adhesion of leukocytes was not observed with F(ab')₂ of Rb2/4, which recognizes the same molecule as Rb1/9 (Fig. 3B), with F(ab')₂ of Rb2/3, or with F(ab')₂ of W6/32, a MAb that recognizes the major histocompatibility antigen on human leukocytes but not on rabbit EC. Adhesion to unactivated rabbit endothelium was not significantly inhibited by any F(ab')₂ fragments. Polymorphonuclear leukocyte (PMN) adhesion to LPS-activated ECs was not inhibited by Rb1/9 F(ab')₂ under any conditions. Thus, the molecule recognized by Rb1/9 is a mononuclear leukocyte–selective adhesion molecule. Furthermore, assays performed at 4°C suggest that the adhesive mechanism mediated by this molecule does not require metabolic energy or leukocyte activation and thus differs from the mechanism by which leukocyte CD11a/CD18 (LFA-1) interacts with its endothelial counter-receptor ICAM-1 (8). The inability of Rb1/9 F(ab')₂ to inhibit adhesion at 37°C suggests that other adhesion mechanisms are also operative at this temperature.

Rb1/9 specifically immunoprecipitated two polypeptides from total cell lysates of biosynthetically labeled, LPS-activated EC monolayers. These polypeptides had relative molecular sizes of 118 and 98 kD on SDS–polyacrylamide gel electrophoresis (SDS-PAGE) under reducing conditions (Fig. 3A); both were expressed on the EC surface, as determined by surface iodination and immunoprecipitation (Fig. 3A); and both were also recognized by Rb2/4 (Fig. 3B). The two polypeptides were purified from the lungs of LPS-treated rabbits and their NH₂-termini sequenced (9). The NH₂-terminal sequence of the 98-kD polypeptide was found to be FKIETFPESRSLA-QIGDSVSLT, which is homologous (20 of 22 amino acids are identical) to the predicted NH₂-terminal sequence of human VCAM-1—a recently cloned cytokine-inducible member of the immunoglobulin superfamily (10), which had been previously identified as INCAM-110, a 110-kD cyto-

kine-induced human EC surface protein involved in adhesion of certain leukocytes and tumor cells (11). The NH₂-terminal amino acid sequence of the 118-kD polypeptide was found to be identical to that of the 98-kD polypeptide (12), suggesting that both polypeptides are products of a single gene. Thus, we have identified a putative rabbit homolog of human VCAM-1. Molecular cloning of the rabbit molecule should elucidate its full structural relation to human VCAM-1 and establish whether the 118-kD and 98-kD cell surface forms are the result of alternative mRNA splicing or post-translational modifications. The recent identification of an additional immunoglobulin-like

Fig. 2. Effect of F(ab')₂ fragments at 37°C (open bars) and 4°C (solid bars) on the adhesion of leukocytes to rabbit aortic ECs that had been treated with LPS for 18 hours. After LPS treatment, EC monolayers (passage 2) were washed and then incubated for 30 min (37°C or 4°C) with saturating concentrations of F(ab')₂ fragments (5 µg per 0.1 ml of RPMI–1% FBS per microtiter well). BCECF-labeled leukocytes suspended in RPMI containing 1% FBS (2 × 10⁵ cells per 0.1 ml) were added at the appropriate temperature to each well. In 37°C adhesion assays, leukocytes were incubated for 10 min

under static conditions with endothelium; wells were then filled with buffer and sealed, and the plates were inverted and centrifuged (250g for 5 min). Adhesion assays performed at 4°C were 30 min in duration, after which nonadherent leukocytes were removed by sealing and inverting the plates for 20 min. In both 37°C and 4°C assays, leukocyte adhesion to monolayers that had been incubated with F(ab')₂ fragments was compared to adhesion to monolayers treated with control buffer (RPMI–1% FBS); statistical significance was determined with a paired t test (*, $P < 0.05$). The mean ± SD values (triplicate measurements) from one of three experiments are plotted. Human leukemic cell lines—myelomonocytic U937 and THP-1 and promyelocytic HL-60—were obtained from the ATCC. Human leukocytes were isolated from blood of normal donors; MONO and LYMPH (monocytes and lymphocytes, respectively) by elutriation and PMN (polymorphonuclear leukocytes) by density gradient centrifugation (15).
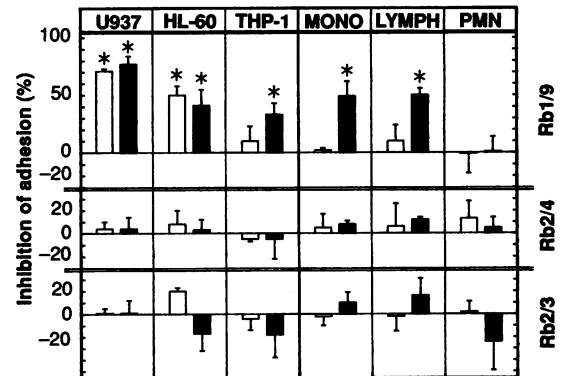
Fig. 3. (A) Specific indirect immunoprecipitation of two polypeptides from rabbit venous EC lysates by MAb Rb1/9. Biosynthetically labeled cells [left panel: (−), control ECs, (+); LPS-activated ECs] and surface-iodinated LPS-activated cells (right panel). MAbs Hu5/3 and E1/C15 (both IgG₁) bind to human, but not rabbit, ECs and did not specifically precipitate polypeptides. EC proteins were biosynthetically labeled with [³⁵S]L-cysteine and [³⁵S]L-methionine for 5 hours (second to seventh hour of LPS treatment) (15). Surface EC proteins were labeled with ¹²⁵I by a glucose oxidase–lactoperoxidase protocol (25). ECs were lysed in 100 mM tris-HCl (pH 7.4), 150 mM NaCl, 5 mM EDTA, 1 mM phenylmethylsulfonyl fluoride, and 0.3% CHAPS, and insoluble material was removed by centrifugation (12,000g for 0.5 hour at 4°C). For immunoprecipitations, EC lysates (~5 × 10⁵ cells per 100 µl) were incubated for 2 to 4 hours at 4°C with 100 µl of MAb culture supernatant and subsequently for 2 to 4 hours with goat antibody to murine IgG coupled to Sepharose 4B (Cappel) (which was first treated with unlabeled lysate to diminish nonspecific adherence of labeled proteins). Lysates of biosynthetically labeled ECs were also precleared with a nonbinding MAb. Antigens that were specifically bound to Sepharose beads were extensively washed, and then subjected to SDS-PAGE under reducing conditions on 5 to 12% linear gradient gels (26). (B) Indirect immunoprecipitation with MAbs (indicated below arrows) performed after twice preclearing surface-iodinated LPS-activated EC lysates with Rb1/9, Rb2/4, or Rb2/3 (×1 and ×2, first and second preclearing, respectively). Rb1/9 and Rb2/4 show reciprocal and specific depletion of antigen, indicating that both MAbs recognize epitopes on the same polypeptides.
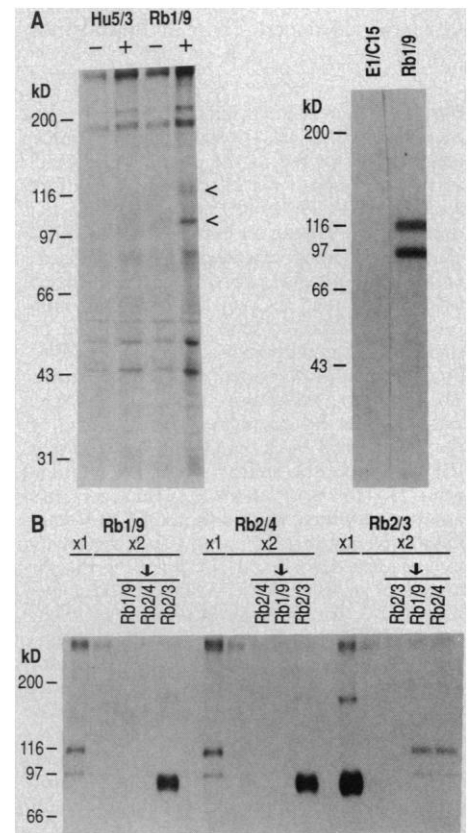
domain in human VCAM-1 that is the result of alternative splicing (13) supports the former possibility.

In contrast to ELAM-1 and ICAM-1 (14), which support PMN adhesion (15), VCAM-1 is mononuclear leukocyte–selective, as determined by MAb inhibition of adhesion to activated human endothelium (11, 16) and expression on COS cells (10). This specificity can be explained by the restricted expression of the VCAM-1 counter-receptor, VLA-4, which is present on monocytes and lymphocytes but not neutrophils (16).

The mononuclear leukocyte–selective adhesion function of the rabbit molecule prompted us to investigate its expression in atherogenesis. Immunohistochemical staining was performed on aortas from rabbits that had been fed a hypercholesterolemic diet and from Watanabe heritable hyperlipidemic (WHHL) rabbits (Fig. 4). Specific staining with Rb1/9 was localized to endothelium covering foam cell–rich aortic intimal lesions at various stages of their development. Of particular interest was staining of ECs both extending beyond the edges of these lesions (Fig. 4A) and focally in regions with very small intimal accumulations of foam cells (Fig. 4B). Nonlesioned aortic endothelium of these hypercholesterolemic animals, as well as endothelium of large arteries and veins of normal rabbits, was uniformly unstained. These findings demonstrate endothelial activation in the setting of atherosclerosis and establish the inducible mononuclear leukocyte endothelial adhesion molecule that is recognized by Rb1/9 as an ATHERO-ELAM. The lesion-selective expression pattern of this molecule may offer a new approach to early diagnosis and lesion-targeted therapeutic intervention in atherosclerosis. Our data also provide a rationale for interfering with VLA-4 function as a therapeutic approach.

VCAM-1 has not yet been described in human atherosclerotic plaques. It is expressed predominantly in postcapillary venular endothelium in inflammatory settings—such as delayed hypersensitivity reactions—and in nonvascular cells, including follicular dendritic cells (11). Human ICAM-1 is found on many cell types, including ECs, monocytes, lymphocytes, follicular dendritic cells, fibroblasts, and epithelial cells (17), and thus may function in a variety of pathophysiological settings; on endothelium, it is expressed constitutively in postcapillary venules and some normal arterioles (17); and in inflammatory reactions, it is upregulated predominantly in venular endothelium (18). Lesion-localized endothelial expression of ICAM-1 in human atherosclerosis has not been described. ELAM-1 is expressed only by endothelium of venules and veins in pathophysiological settings involving inflammation (18, 19); it has not been detected in a variety of human atherosclerotic lesions, ranging from early fatty streaks to advanced plaques (20). Thus, specific leukocyte adhesion molecules can be differentially expressed by various cell types, including arterial versus venous endothelium, and suggest that the lesion-localized expression pattern of the putative rabbit VCAM-1 may have pathogenic significance.

The endothelial lining normally maintains homeostasis at the vessel wall–blood interface (21). Endothelial dysfunction (22) has been implicated in the vasospastic and thrombotic complications that are evident in advanced atherosclerosis. Induction of an adhesion molecule early in atherogenesis may also be considered a manifestation of endothelial dysfunction, in that it results in an abnormally hyperadhesive EC surface. This alone, or in conjunction with other localizing mechanisms—including vessel wall–derived chemoattractants (23)—could promote mononuclear leukocyte recruitment. The mononuclear leukocyte selectivity of the induced adhesion molecule is consistent with the accumulation of monocytes and lymphocytes (but not PMNs) that is observed during atherogenesis (1). In vivo testing of the function of this ATHERO-ELAM should help to establish whether the temporal and spatial patterns of its expression are determinants of lesion initiation and progression. Defining the molecular mechanisms that regulate the expression of this and other ATHERO-ELAMs, and their relations to known risk factors for atherosclerosis, such as hypercholesterolemia (24), may provide new insights into the pathogenesis of this complex disease.

Fig. 4. Immunohistochemical staining of rabbit aortas. (**A** and **B**) Rb1/9 staining of atherosclerotic lesions located in the descending thoracic aorta from rabbits fed a 1% cholesterol diet for 9 weeks. (A) Rb1/9 staining was detected in ECs overlying the edge of an intimal foam cell lesion (IL). EC staining extended into the adjacent uninvolved aorta (UA) (arrowhead marks edge of lesion). (A, inset) ECs in the remaining uninvolved aorta failed to stain with Rb1/9, but did stain with goat antibodies to human von Willebrand Factor (1:3000 dilution of IgG; Atlantic Ab), which is a constitutive EC marker. In serial sections, ECs did not stain with a nonbinding, isotype-matched MAb, E1/C15. (FC, foam cells; IEL, internal elastic lamina; bar corresponds to 50 μm.) (B) In early lesions consisting of small numbers of intimal foam cells, focal Rb1/9 staining was evident (bar, 100 μm). (**C**) ECs overlying well-developed, foam cell–rich lesions in the aortic arch of an 18-week-old WHHL rabbit stained with Rb1/9 (bar, 10 μm). In a variety of lesions examined in both dietary hypercholesterolemic and WHHL rabbits, individual ECs showed different staining intensities; most intense staining was at the edges of lesions. Immunoperoxidase staining was performed on 4- to 6-μm frozen sections that had been fixed at −20°C for 5 min in acetone. Sections were incubated (22°C) in succession with tissue culture supernatants containing Rb1/9 (2 hours), biotinylated horse antibodies to murine IgG (1 hour), and avidin-biotin peroxidase complexes (45 min) (Vector Labs.). Peroxidase was visualized with 3-amino-9-ethylcarbazole (Sigma) and sections were counterstained with Gill's hematoxylin. The MAbs to rabbit EC, including Rb1/9, do not recognize epitopes on normal or activated human endothelium in culture or in tissue sections.
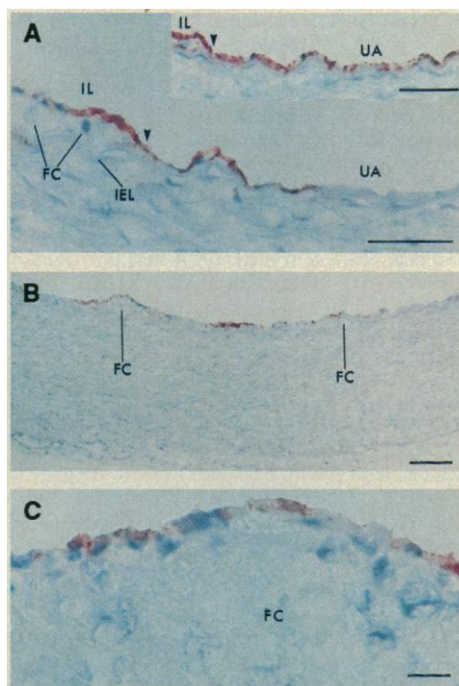
REFERENCES AND NOTES

1. R. Ross, *N. Engl. J. Med.* **314**, 488 (1986); J. M. Munro and R. S. Cotran, *Lab. Invest.* **58**, 249 (1988); G. K. Hansson, L. Jonasson, P. S. Seifert, S. Stemme, *Arteriosclerosis* **9**, 567 (1989).
2. L. N. Walker, M. A. Reidy, D. E. Bowyer, *Am. J. Pathol.* **125**, 450 (1986).
3. T. Watanabe *et al.*, *Lab. Invest.* **53**, 80 (1985); L. M. Buja, T. Kita, J. L. Goldstein, Y. Watanabe, M. S. Brown, *Arteriosclerosis* **3**, 87 (1983); M. E. Rosenfeld, T. Tsukada, A. M. Gown, R. Ross, *ibid.* **7**, 9 (1987).
4. Rabbit aortas and inferior venae cavae were freshly harvested in Dulbecco's phosphate-buffered saline, the adventitia were removed under sterile conditions, and the vessels were everted and tied to sterile pipettes. ECs were isolated from these everted blood vessels with 0.2 or 0.4% collagenase (type I; Worthington), respectively, and cultured on gelatin-coated tissue culture plastic in Medium 199 (Hanks salts, M.A. Bioproducts) containing 20% fetal bovine serum (FBS), EC mitogen (10 to 20 μg/ml) (Biomedical Technologies), and porcine intestinal heparin (20 to 40 μg/ml) (Sigma; grade I). The concentrations of EC mitogen and heparin were reduced as endothelial monolayers approached confluence. Cells were passaged with the use of trypsin and EDTA, and they grew to form confluent monolayers with morphological and functional features that are characteristic of differentiated endothelium.
5. Quantitative adhesion assays were performed in microtiter plates as described by F. W. Luscinskas *et al.* (15). Leukocytes labeled with 2'-7'-bis-(2-car-

boxyethyl-5-(46)carboxyfluorescein (BCECF) and suspended in RPMI containing 1% FBS (2 × 10⁵ cells per 0.2 ml per well) were allowed to adhere to EC monolayers for 10 min at 37°C. Wells were then filled with buffer, and the plates were sealed, inverted, and centrifuged (250g for 5 min at 22°C).

6. P. Harris and P. Ralph, *J. Leuk. Biol.* **37**, 407 (1985).
7. MAbs were generated by fusing NS-1 myeloma cells with spleen cells from mice that had been immunized with LPS-treated (for 5 hours) inferior vena caval ECs. Cell surface binding assays were performed at 4°C on viable EC monolayers with saturating concentrations of MAb supernatants and fluorescein-conjugated F(ab')₂ fragments of goat antibodies to murine IgG (Caltag Labs). Fluorescence levels were determined with an automated plate reader (Pandex; Baxter Healthcare), and specific MAb binding was determined by subtracting fluorescence values obtained with IgG₁ antibodies that do not bind to rabbit ECs [~50 relative fluorescence units (RFU)].
8. M. L. Dustin and T. A. Springer, *Nature* **341**, 619 (1989).
9. Polypeptides were purified by Rb1/9 immunoaffinity chromatography (Affi-Gel Hz; Bio-Rad) and SDS-PAGE from cell membranes prepared from the lungs of ten rabbits, which had been killed 4 hours after an intravenous injection of LPS (100 μg per kilogram of body mass). Polypeptides were then transferred to an Immobilon-P membrane (Millipore), and NH₂-terminal sequences were determined from excised Coomassie blue–stained bands by phenyl isothiocyanate degradation cycles on an automated gas-phase sequencer (Applied Biosystems) [N. LeGendre and P. Matsudaira, in *A Practical Guide to Protein and Peptide Purification for Microsequencing*, P. Matsudaira, Ed. (Academic Press, San Diego, 1989), pp. 49–69]. Abbreviations for the amino acid residues are: A, Ala; C, Cys; D, Asp; E, Glu; F, Phe; G, Gly; H, His; I, Ile; K, Lys; L, Leu; M, Met; N, Asn; P, Pro; Q, Gln; R, Arg; S, Ser; T, Thr; V, Val; W, Trp; and Y, Tyr.
10. L. Osborn *et al.*, *Cell* **59**, 1203 (1989).
11. G. E. Rice and M. P. Bevilacqua, *Science* **246**, 1303 (1989); G. E. Rice, J. M. Munro, M. P. Bevilacqua, *J. Exp. Med.* **171**, 1369 (1990).
12. M. I. Cybulsky *et al.*, *Am. J. Pathol.*, in press; T. Polte, W. Newman, T. V. Gopal, *Nucleic Acids Res.* **18**, 5901 (1990).
13. M. I. Cybulsky, J. W. U. Fries, M. A. Gimbrone, Jr., T. Collins, in preparation.
14. M. P. Bevilacqua, S. Stengelin, M. A. Gimbrone, Jr., B. Seed, *Science* **243**, 1160 (1989); T. A. Springer, *Nature* **346**, 425 (1990).
15. F. W. Luscinskas, A. F. Brock, M. A. Arnaout, M. A. Gimbrone, Jr., *J. Immunol.* **142**, 2257 (1989); M. P. Bevilacqua, J. S. Pober, D. L. Mendrick, R. S. Cotran, M. A. Gimbrone, Jr., *Proc. Natl. Acad. Sci. U.S.A.* **84**, 9238 (1987); C. W. Smith *et al.*, *J. Clin. Invest.* **82**, 1746 (1988).
16. M. J. Elices *et al.*, *Cell* **60**, 577 (1990); B. R. Schwartz, E. A. Wayner, T. M. Carlos, H. D. Ochs, J. M. Harlan, *J. Clin. Invest.* **85**, 2019 (1990).
17. M. L. Dustin, R. Rothlein, A. K. Bhan, C. A. Dinarello, T. A. Springer, *J. Immunol.* **137**, 245 (1986); R. J. Faull and G. R. Russ, *Transplantation* **48**, 226 (1989).
18. R. S. Cotran *et al.*, *J. Immunol.* **140**, 1883 (1988); J. M. Munro, J. S. Pober, R. S. Cotran, *Am. J. Pathol.* **135**, 121 (1989).
19. R. S. Cotran, M. A. Gimbrone, Jr., M. P. Bevilacqua, D. L. Mendrick, J. S. Pober, *J. Exp. Med.* **164**, 661 (1986).
20. J. M. Munro, J. S. Pober, R. S. Cotran, personal communication.
21. M. A. Gimbrone, Jr., in *Vascular Endothelium in Hemostasis and Thrombosis*, M. A. Gimbrone, Jr., Ed. (Churchill Livingstone, Edinburgh, 1986), pp. 1–13; R. J. Gryglewski, R. M. Botting, J. R. Vane, *Hypertension* **12**, 530 (1988).
22. M. A. Gimbrone, Jr., in *Arteriosclerosis V. Proceedings of the Fifth International Symposium on Atherosclerosis*, A. M. Gotto, Jr., L. C. Smith, B. Allen, Eds. (Springer-Verlag, New York, 1980), pp. 415–425.
23. R. G. Gerrity, J. A. Goss, L. Soby, *Arteriosclerosis* **5**, 55 (1985); J. A. Berliner *et al.*, *ibid.* **6**, 254 (1986); A. J. Valente, D. T. Graves, C. E. Vialle-Valentin,

R. Delgado, C. J. Schwartz, *Biochemistry* **27**, 4162 (1988); M. T. Quinn, S. Parthasarathy, D. Steinberg, *Proc. Natl. Acad. Sci. U.S.A.* **85**, 2805 (1988).
24. D. Steinberg, S. Parthasarathy, T. E. Carew, J. C. Khoo, J. L. Witztum, *N. Engl. J. Med.* **320**, 915 (1989).
25. A. L. Hubbard and Z. A. Cohn, *J. Cell Biol.* **64**, 438 (1975).
26. U. K. Laemmli, *Nature* **227**, 680 (1970).
27. We thank J. Baker and W. Henzel for NH₂-terminal amino acid sequencing; J. Kiely and V. Davis for

---

Human Immunodeficiency Virus Infection of Human-PBL-SCID Mice

DONALD E. MOSIER, RICHARD J. GULIZIA, STEPHEN M. BAIRD, DARCY B. WILSON,* DEBORAH H. SPECTOR, STEPHEN A. SPECTOR

Severe combined immunodeficient (SCID) mice reconstituted with human peripheral blood leukocytes (hu-PBL-SCID mice) have inducible human immune function and may be useful as a small animal model for acquired immunodeficiency syndrome (AIDS) research. Hu-PBL-SCID mice infected with human immunodeficiency virus-1 (HIV-1) contained virus that was recoverable by culture from the peritoneal cavity, spleen, peripheral blood, and lymph nodes for up to 16 weeks after infection; viral sequences were also detected by in situ hybridization and by amplification with the polymerase chain reaction (PCR). Mice could be infected with multiple strains of HIV-1, including LAV-1/Bru, IIIB, MN, SF2, and SF13. HIV-1 infection affected the concentration of human immunoglobulin and the number of CD4⁺ T cells in the mice. These results support the use of the hu-PBL-SCID mouse for studies of the pathogenesis and treatment of AIDS.

THE NEED FOR BETTER SMALL ANImal models for research into the causes and prevention of AIDS has prompted the development of two experimental systems (*1, 2*) that involve the transplantation of human lymphoid cells or tissue into mice with the SCID mutation (*3*). When adult human peripheral blood leukocytes (PBLs) are transferred to SCID mice, thus creating hu-PBL-SCID mice, the human T and B lymphocytes survive, human immunoglobulin is produced, and secondary antibody responses can be elicited (*1, 4*). Implantation of human fetal lymphoid tissue into SCID mice creates SCID-hu mice (*2*); such mice support HIV-1 RNA transcription and lesser expression of viral proteins (*5*). We have recovered HIV-1 from the peritoneal cells, lymphoid organs, and blood of hu-PBL-SCID mice infected with either cell-free or cell-associated virus for up

to 16 weeks after infection. HIV-1 infection with high virus loads led to an initial increase, then a reduction in human immunoglobulin production in hu-PBL-SCID mice and changes in the number of CD4⁺ T cells in many mice. We conclude that HIV-1 is infectious in the hu-PBL-SCID model, and that infection results in changes in human lymphocyte function consistent with those seen in HIV-1–infected individuals.

Hu-PBL-SCID mice were generated by reconstituting adult SCID mice by intraperitoneal injection of 1 × 10⁷ to 4 × 10⁷ PBLs from donors that were negative for antibodies to Epstein-Barr virus (EBV) capsid antigens. [EBV-seronegative donors were used to prevent the possible development of EBV-associated B cell lymphoproliferative disease (*1, 6*) and to eliminate one potential cofactor in HIV-1 pathogenesis.] Mice were challenged by intraperitoneal injection (*7*) either with 10¹ to 10⁵ median tissue culture infectious doses (TCID₅₀) of cell-free virus (144 mice) or with virus-infected autologous T lymphoblasts (27 mice) (*8*) and evaluated for HIV-1 infection by (i) culture of hu-PBL-SCID lymphoid tissue with fresh human PBLs (*9*), (ii) in situ cytohybridization with a full-length cDNA probe for the IIIB strain of HIV-1 (HIV-1$_{\text{IIIB}}$) (*10*), and (iii) amplification of HIV-1 *gag* sequences by the polymerase chain reaction (PCR)

D. E. Mosier, R. J. Gulizia, D. B. Wilson, Division of Immunology, Medical Biology Institute, La Jolla, CA 92037.
S. M. Baird, Veterans Administration Medical Center, La Jolla, CA 92161, and Department of Pathology, University of California at San Diego, La Jolla, CA 92093.
D. H. Spector, Department of Biology, University of California at San Diego, La Jolla, CA 92093.
S. A. Spector, Department of Pediatrics, University of California at San Diego, La Jolla, CA 92093.

*Present address: La Jolla Institute of Experimental Medicine, La Jolla, CA 92037.